2024 American Control Conference (ACC)
July 8-12, 2024. Toronto, Canada

Flow sensing and feedback control for maintaining school cohesion in uncoordinated flapping swimmers

Haotian Hang, Sina Heydari and Eva Kanso [1]

Abstract— **Fish often swim in schools. Flow interactions are thought to be beneficial for schooling. Recent work shows that flow interactions cause a pair of free inline swimmers, flapping at the same frequency, to passively stabilize at discrete locations relative to each other and that these passively stable formations are energetically beneficial. However, the stability of these formations is sensitive to finite mismatch in flapping frequencies. Here, we propose a local flow sensing model and feedback controller that stabilize a pair of frequency-uncoordinated swimmers into a cohesive formation. Our findings bear relevance to understanding fish collective behavior and for designing bio-inspired underwater robotics.**

I. INTRODUCTION

Fish schools are ubiquitous. Half of the known fish species exhibit schooling behavior during some phase of their life cycle [1]. Flow interactions are thought to provide hydrodynamic benefits to school members [2], [3], [4], but a direct assessment of this hypothesis is challenging because of the complexity of resolving the unsteady flows in multiple interacting fish ([5], [6]) and of deciphering the sensing and feedback mechanisms that individual fish use when schooling ([7], [8], [6], [9]). To simplify the problem, physical ([10], [11], [12], [13], [14], [15]) and mathematical ([16], [17], [18], [19]) models considered flapping foils interacting via their own self-generated flows, with no sensing or ability to adjust their flapping motion. Pairs of foils undergoing prescribed heaving [14], [15] or pitching [18], [19] oscillations at the same frequency and amplitude were placed in tandem and allowed to swim freely. Experiments and simulations proved that flow interactions stabilize the pair at constant spacing relative to each other [14], [15], [18], [19]. These emergent formations are both stable and energetically beneficial [18], [19]. The relative distance between leader and follower in these emergent formations varies linearly with the difference in flapping phase [14], [19]. This linear phase-distance relationship was also observed in live fish and associated with energy saving [20].

Most studies focused on coordinated swimmers that flap at the same amplitude and frequency. In [14], pairs of uncoordinated swimmers were considered. The authors examined, experimentally and in reduced-order models, the stability of the emergent formation subject to mismatch in flapping amplitude and/or frequency. Two swimmers coordinated in frequency with minor mismatch in amplitude can stabilize passively and swim together in a coherent formation. However, subtle frequency mismatch leads to instability and loss of school cohesion.

In this work, to stabilize the formation of a pair of swimmers flapping at different frequencies, we devise a feedback controller based on local flow sensing inspired by [21]. We consider frequency control instead of amplitude control for two reasons. First, as suggested in [22], when fish try to accelerate or decelerate, they typically adjust their undulation frequency while maintaining the same body deformation amplitude for optimal hydrodynamic performance. Thus, developing a frequency controller is of biological relevance. Secondly, frequency is more detrimental to the stability of emergent formation as demonstrated in [14].

The rest of this paper is organized as follows. In Sec. II, we present the reduced-order model employed in [14] and analyze the stability of open-loop dynamics, with no feedback control. In Sec. III, we explore local flow sensing strategies that a follower can use to estimate the frequency of the leader. In Sec. IV, we describe the design and performance of the proposed controller. We summarize our findings and discuss future directions in Sec. V.

II. MATHEMATICAL MODEL

We employed a time-delayed particle model [14] to describe a pair of flow-coupled oscillating swimmers (Fig. 1). Each swimmer is modeled as a point mass that oscillates in the y-direction to propel itself in the x-direction. Let $y_1 = A_1 \sin(2\pi f_1 t)$ and $y_2 = A_2 \sin(2\pi f_2 t - \phi)$ denote the transverse oscillations of the leader and follower, respectively, where A_i, f_i, $i = 1, 2$, are the amplitude and frequency of oscillations, and ϕ is the phase difference between two swimmers, and let $x_1(t)$ and $x_2(t)$ denote their swimming motion.

Each foil experiences a thrust force proportional to the square of its vertical velocity relative to the ambient fluid and a drag force proportional to the square of its horizontal velocity relative to the ambient fluid [11], [23], [24], [14], namely,

$$F_i = C_T(\dot{y}_i - v(x_i))^2, \quad D_i = C_D(\dot{x}_i - u(x_i))^2, \qquad (1)$$

where $u(x_i)$ and $v(x_i)$ are the components of the fluid velocity in the x and y-directions at the location of the i^{th} swimmer, and C_T and C_D are the thrust parameter and drag parameter, respectively.

The leader swims into still water, which means $u(x_1) = v(x_1) = 0$ and creates a transverse wake $(u(x_2) = 0)$ in

[1]Eva Kanso is a Professor in the Department of Aerospace and Mechanical Engineering and the Department of Physics and Astronomy at the University of Southern California, 3650 McClintock Ave, Los Angeles, California 90089, USA Kanso@usc.edu. Haotian Hang and Sina Heydari are present and former PhD students. Sina Heydari is now a lecturer in the Department of Mechanical Engineering, Santa Clara University. Supplementary movie is available at $https://youtu.be/E_o3o2L4oTI$.

979-8-3503-8265-5/$31.00 ©2024 AACC

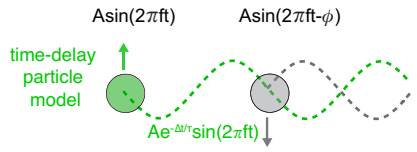

Fig. 1. Schematics of time delayed particle model. Each swimmer is modeled as particles oscillating in vertical direction $A\sin(2\pi ft)$ and left a wake which decays exponentially with time [14], [19].

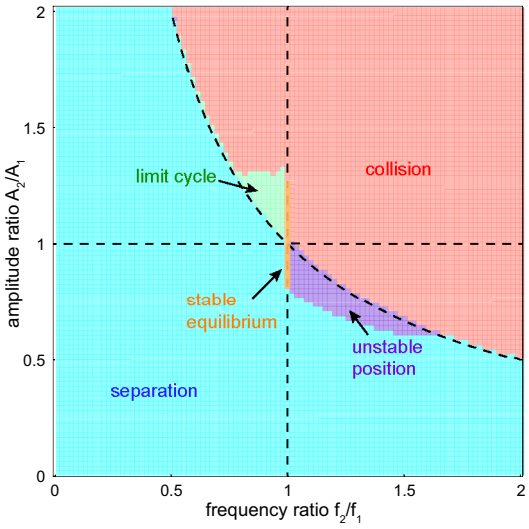

Fig. 2. Parametric study of the model behavior over frequency ratio and amplitude ratio. Other parameters are fixed at $\tau = 1$, $A_1 = \sin 15°$, $f_1 = 1$, $\phi = 0$. Reproduced independently from [14].

the fluid environment for the follower to interact with. The transverse velocity of the leader's wake at its present location is the same as its oscillatory speed $\dot{y}_1(t)$. This wake decays exponentially with time $e^{-\Delta t/\tau}$, where Δt denotes the time passed since the leader occupied that location. The parameter τ depends on the scale of the problem: larger τ models weaker viscous effect or larger Reynolds number. Say at $t-\Delta t$, the leader occupied the position where the follower is now located $x_1(t-\Delta t) = x_2(t)$. The follower thus interacts with a transverse wake of velocity $e^{-\Delta t/\tau}\dot{y}_1(t-\Delta t)$. The equations of motion for both swimmers $(i = 1, 2)$ are given by

$$m\ddot{x}_i = -F_i + C_D\dot{x}_i^2, \tag{2}$$

where

$$\begin{aligned} F_1 &= C_T\dot{y}_1^2, \\ F_2 &= C_T(\dot{y}_2(t) - e^{-\Delta t/\tau}\dot{y}_1(t-\Delta t))^2, \\ x_1(t-\Delta t) &= x_2(t). \end{aligned} \tag{3}$$

Here, m is the mass of each swimmer. The average swimming speed of the leader is solved analytically as $U_1 = \pi A_1 f_1\sqrt{2C_T/C_D}$, but the swimming speed of the follower is solved numerically via Runge–Kutta methods. Solutions are shown in Fig. 3, where the separation distance d between the two swimmers is scaled by the wavelength of the wake left by leader $\lambda = U_1/f_1$.

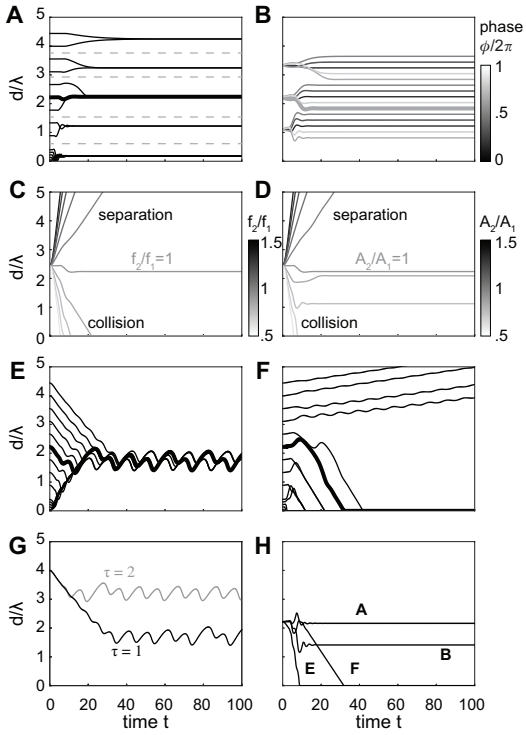

Fig. 3. Scaled distance as a function of time for different parameter values. **A** $f_2/f_1 = 1$, $A_2/A_1 = 1$, $\tau = 1$, $\phi = 0$ with different initial distance; **B** $f_2/f_1 = 1$, $A_2/A_1 = 1$, $\tau = 1$ with phase ϕ ranges from 0 to 2π; **C** $f_2/f_1 \in [0.5, 1.5]$, $A_2/A_1 = 1$, $\tau = 1$; **D** $f_2/f_1 = 1$, $A_2/A_1 \in [0.5, 1.5]$, $\tau = 1$; **E** $f_2/f_1 = 0.9$, $A_2/A_1 = 1.2$, $\tau = 1$; **F** $f_2/f_1 = 1.1$, $A_2/A_1 = 0.9$, $\tau = 1$; **G** $f_2/f_1 = 0.9$, $A_2/A_1 = 1.2$, $\tau = 1, 2$; **H** $\tau = \infty$ with cases from **A**, **B**, **E**, and **F**. Other parameters are kept the same as $C_D = 0.25$, $C_T = 0.96$, $m = 1.325g/cm^2$, $A_1 = \sin 15°$, $f_1 = 1$ [14], [19].

Following [14], we explored the behavior of the two swimmers over the entire space of frequency and amplitude ratios f_2/f_1 and A_2/A_1 (Fig. 2). For each set of parameter values, we calculated the separation distance between the leader and follower for 16 different initial conditions ranging from $d_0/\lambda = 1$ to $d_0/\lambda = 16$. We found, consistent with [14], that the swimmers reach one of five characteristic behaviors: (1) reach a stable formation and swim together in a relative equilibrium; (2) always separate; (3) always collide; (4) separate or collide based on initial conditions; or (5) reach stable periodic limit cycles.

It is instructive to show representative trajectories for each of the five behaviors identified in Fig. 2. In Fig. 3A, we considered the case when the frequency and amplitude of two swimmers are the same and the two swimmers oscillate inphase ($\phi = 0$). Depending on the initial separation distance, the follower positions itself at one of multiple relative equilibria, consistent with [14], [18]. Each equilibrium has its own basin of attractions, as illustrated by dashed grey lines. When the swimmers flap at a phase lag relative to each other ($\phi \neq 0$), the equilibria shift following a linear phase-distance relationship $\phi/2\pi = d/U_1 f_1 + \text{const}$ (Fig. 3B) [14], [20], [19].

We next considered cases when the follower flaps at a mis-

match in either amplitude or frequency relative to the leader (Fig. 3C and D). When the follower flaps at larger frequency ($f_2/f_1 > 1$) or amplitude ($A_2/A_1 > 1.2$), it always collides with the leader regardless of initial conditions. When the follower flaps at smaller frequency ($f_2/f_1 < 1$) or amplitude ($A_2/A_1 < 0.8$), the two swimmers always separate. The stability of the formation is more sensitive to differences in frequency; indeed, there is a big margin of amplitude mismatch ($A_2/A_1 \in [0.8, 1.2]$) for which uncoordinated swimmers can swim together cohesively, but a tiny amount of frequency mismatch makes the school unstable (Fig. 2).

The separation or collision can be explained intuitively as follows. Higher amplitude (higher frequency) generates higher thrust and vice versa (Eq. 2). However, frequency mismatch brings additional and unique effects. It introduces a time-dependent phase shift $\phi(t) = (f_1 - f_2)t$. When the frequency of the follower is smaller than that of the leader ($f_2 < f_1$), the phase ϕ constantly increases with time, and given the aforementioned linear phase-distance relationship, the equilibrium distance d also increases. That is, $f_2 < f_1$ increases phase difference and decreases thrust on the follower, both lead to an increased separation between leader and follower. For $f_2 > f_1$, phase decreases and thrust increases, and both effects lead to collision.

We lastly considered two cases when both amplitude and frequency are mismatched (Fig. 3E,F). In Fig. 3F, the frequency of the follower is larger ($f_2 > f_1$) and the vertical velocity of the follower is smaller ($A_2 f_2 < A_1 f_1$). Here, depending on initial conditions, the follower either separates from the leader or collides with the leader. Combinations of amplitude and frequency ratios that lead to either collision or separation based on initial conditions are categorized as unstable [14] (Fig. 2).

When the frequency of the follower is smaller than that of the leader ($f_2 < f_1$) but the transverse velocity of the follower is larger ($A_2 f_2 > A_1 f_1$), they form a stable limit cycle (Fig. 3E). When the follower is close to the leader, the leader's wake strongly affects the follower's motion and the phase effect discussed earlier pushes the follower away from the leader. When the separation distance is larger, exponential decay of the wake makes the motion of the follower less affected by the wake. Because the transverse velocity of the follower is larger, its self-propelled velocity is larger than the leader. Thus, the follower swims forward and forms the limit cycle. The limit cycle is a global attractor in the system because it only appears at the position where the magnitude of the phase effect and thrust effect are close. Note that the relative equilibria of the coordinated swimmers ($A_2/A_1 = 1$ and $f_2/f_1 = 1$) are independent of τ (Fig. 3H), but the limit cycles that emerge in the uncoordinated swimmers are scale-dependent; they depend on the value of τ (Fig. 3G). When considering the limit $\tau \to \infty$, the limit cycle disappears (Fig. 3H).

III. FLOW SENSING MODEL

The parametric study in Fig. 2 shows that the pair of swimmers lose cohesion when the follower is flapping at the same amplitude ($A_2/A_1 = 1$) but different frequency ($f_2/f_1 \neq 1$) from the leader. To form a coherent school, an intuitive idea is for the follower to try to match its own frequency with the frequency of the leader. However, the frequency of the leader f_1 is unknown to the follower. Thus, we need to estimate it based on the follower's local information. The follower has access to its own swimming velocity $\dot{x}_2(t)$, the flow velocity at its own location $e^{-\Delta t/\tau}\dot{y}_1(t-\Delta t)$, and the hydrodynamic force $F_2(t)$ acting on it. Here we discuss scenarios by which the follower, from this local information, can estimate the flapping frequency f_1 of the leader.

A. SIMPLIFIED SENSING SCENARIOS

We first considered a one-way coupled problem in which the follower probes the flow velocity in the wake of the leader, but its swimming motion is not influenced by the leader's wake. Thus, the swimming speed of the follower is given by $U_2 = \pi A_2 f_2 \sqrt{2C_T/C_D}$ and its motion is given by $x_2(t) = -U_2 t$. The flow velocity left by the leader is given by $v(x,t) = 2\pi A_1 f_1 e^{-(x+U_1 t)/U_1 \tau} \cos(2\pi f_1 x/U_1)$. The signal sensed by the follower as a function of time is $v(x_2(t),t) = 2\pi A_1 f_1 e^{-(-U_2 t + U_1 t)/U_1 \tau} \cos(2\pi f_1 U_2/U_1 t)$. Thus, the dominant frequency is $f_1 U_2/U_1 = f_2 A_2/A_1$. Under this scenario, the follower cannot decode information about the leader's oscillatory frequency.

We next considered that both swimmers are tethered, in which the gap distance $d(t)$ between them is kept constant d, and the incoming flow velocity is the self-propelled swimming speed of the leader U_1. Here, $\Delta t = d/U_1$ is a constant. The flow velocity sensed by the follower is $2\pi A_1 f_1 e^{-d//U_1\tau} \cos(2\pi f_1 (t - d/U_1))$, in which the frequency of leader f_1 can be decoded by a frequency analysis. Alternatively, if the follower senses the fluid force instead of flow velocity, the force can be decomposed can be represented in a Fourier series expansion, with four Fourier modes $|f_1 - f_2|$, $f_1 + f_2$, $2\max(f_1, f_2)$, $2\min(f_1, f_2)$, which encode the leader's frequency f_1. In fact, the follower only needs the first two Fourier modes are sufficient to decode the frequency of the leader.

B. FLOW SENSING DURING FREE SWIMMING

The simplified scenarios discussed above are insufficient to decode the frequency of the leader while swimming freely. To this end, we considered the original two-way coupled problem in Eq. (2). We used the flow velocity $v(x_2(t),t)$ at the location of the follower as sensory cue and took the Fourier series expansion of this flow velocity. We considered the limit of high Reynolds number ($\tau \to \infty$) to ensure long enough signal. Fig. 4A,B shows four typical examples. When the follower's frequency f_2 is smaller than that of the leader and the leader frequency is normalized to $f_1 = 1$, the frequency of the dominant mode is nearly independent of the follower's frequency (Fig. 4A): for $f_2 = 0.6$ and $f_2 = 0.7$, respectively, the dominant mode has frequency $f_s = 1.15$ and $f_s = 1.18$ (the follower frequency f_2 is reflected in the second mode of flow velocity). When the follower's frequency f_2 is larger than the leader, the first mode only

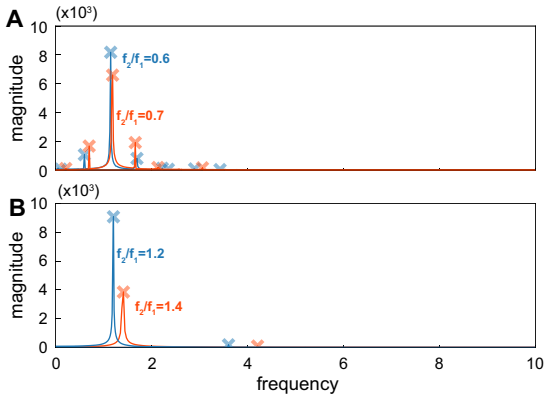

Fig. 4. Fourier analysis of flow velocity sensed by the follower. **A.** The follower's frequency is smaller than that of the leader ($f_2/f_1 = 0.6, 0.7$). **B.** The follower's frequency is larger than that of the leader ($f_2/f_1 = 1.2, 1.4$).

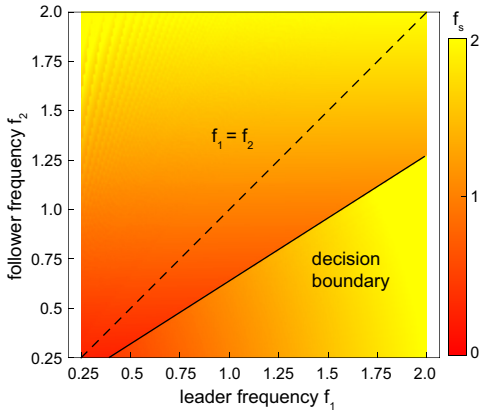

Fig. 5. Dominant frequency of sensed flow velocity f_s as a function of leader frequency f_1 and follower frequency f_2.

reflects the frequency of the follower $f_s \approx f_2$ (Fig. 4B): for $f_2 = 1.2$ and $f_2 = 1.4$, respectively, the dominant mode has frequency $f_s = 1.2$ and $f_s = 1.4$.

We set out to probe whether $f_2/f_1 = 1$ indeed determines the boundary between when the dominant Fourier mode f_s of $v(x_2(t), t)$ reflects either f_1 or f_2. We discretized the frequency space (f_1, f_2) between $([0.25, 2] \times [0.25, 2])$ using a 175×175 grid and at each grid point, we solved the coupled time-delay system in Eq. (2) for a time interval from $[0, 100]$ using a timestep $\mathrm{d}t = 10^{-3}$. We evaluated $v(x_2(t), t)$ over the entire time interval and calculated the dominant Fourier mode. Results are shown as a colormap over the (f_1, f_2) space in Fig. 5. We found that the boundary between whether f_1 or f_2 are reflected in the dominant mode f_s is not $f_1 = f_2$ (dashed line in Fig. 5). Instead, it is a line with a smaller slope (solid line). Below this line, f_s is close but not exactly equal to f_1. Above this line, f_s is equal to f_2 (up to a small numerical error $< 10^{-8}$). To understand this transition in f_s at the solid line, we went back to analyze the equation of motion Eq. (2) in an effort to determine analytically the dominant frequency.

C. FREQUENCY ANALYSIS

To simplify the equations of motion, we assumed that the leader is moving at a constant speed U_1 equal to its time-average speed $\dot{x}_1(t) = -U_1$. Substituting into Eq. (2), we obtained the following decoupled system of equation

$$\begin{aligned} m\ddot{x}_2 =& -F_2 + D_2, \quad D_2 = C_D(\dot{x}_2)^2 \\ F_2 =& C_T(2\pi A_2 f_2 \cos(2\pi f_2 t - \phi) \\ & - 2\pi A_1 f_1 e^{-\Delta t/\tau} \cos(2\pi f_1(t - \Delta t)))^2 \\ \Delta t =& x_2/U_1 + t \end{aligned} \tag{4}$$

We expanded the expression for the force F_2, ignored the high frequency $(f_1 + f_2)$ term (in simulation, we checked that ignoring this term does not influence the dynamics of the problem), and took the limit of $\tau \to \infty$:

$$\begin{aligned} F_2 =& C_1 + C_2 + C_1 \cos(4\pi f_2 t - 2\phi) \\ & + C_2 \cos(4\pi f_1 t - 2t - 2x_2/U_1) \\ & - C_3 \cos(2\pi(f_1 - f_2)t - t - x_2/U_1 + \phi), \end{aligned} \tag{5}$$

where the coefficients $C_1 = 2\pi^2 A_2^2 f_2^2 C_T$, $C_2 = 2\pi^2 A_1^2 f_1^2 C_T$, $C_3 = 4\pi^2 A_1 A_2 f_1 f_2 C_T$ are introduced to simplify the notation.

We assumed that $x_2 = B_0 + B_1 t + B_2 \cos(B_3 t)$ at steady state, where B_0, B_1, B_2, and B_3 are unknown constants representing the follower's initial location, average speed, and amplitude, and frequency of oscillation speed. Substituting into Eq. (5), we get

$$\begin{aligned} F_2 =& C_1 + C_2 + C_1 \cos(4\pi f_2 t - 2\phi) \\ & + C_2 \cos[(4\pi f_1 - 2 - 2B_1/U_1)t \\ & - 2B_0/U_1 - 2B_2 \cos(B_3 t)/U_1] \\ & - C_3 \cos[(2\pi f_1 - 2\pi f_2 - 1 - B_1/U_1)t \\ & - B_0/U_1 - B_2 \cos(B_3 t)/U_1 + \phi] \end{aligned} \tag{6}$$

The complexity of this equation comes from the composite trigonometric functions: the unknown function x_2 is inside the cos function, e.g. the presence of term $\cos(B_2 \cos(B_3 t)/U_1)$. Fourier expansion of $\cos[B_2 \cos(B_3 t)]$ gives $J_{B_2}(0) - 2J_{B_2}(2)\cos(2B_3 t) + \text{h.o.t}$, where J_α denotes Bessel functions of the first kind. In this expansion, using the first two terms is a good estimation of the nested trigonometric functions. As such, Eq. (6) can be further simplified to

$$\begin{aligned} F_2 =& C_1 + C_2 + C_1 \cos(4\pi f_2 t - 2\phi) \\ & + C_2[J_{2B_2}(0) - 2J_{2B_2}(2)\cos(2B_3 t)] \\ & \cos[(4\pi f_1 - 2 - 2B_1/U_1)t - 2B_0/U_1] \\ & - C_2[2J_{2B_2}(1)\cos(B_3 t) - 2J_{2B_2}(3)\cos(3B_3 t)] \\ & \sin[(4\pi f_1 - 2 - 2B_1/U_1)t - 2B_0/U_1]\cos(2B_3 t) \\ & - C_3[J_{B_2}(0) - 2J_{B_2}(2)\cos(2B_3 t)] \\ & \cos[(2\pi(f_1 - f_2) - 1 - B_1/U_1)t - B_0/U_1 + \phi] \\ & + C_3[2J_{B_2}(1)\cos(B_3 t) - 2J_{B_2}(3)\cos(3B_3 t)] \\ & \sin[(2\pi(f_1 - f_2) - 1 - B_1/U_1)t - B_0/U_1 + \phi] \end{aligned} \tag{7}$$

From the above equation, when $f_2 > \sqrt{J_{2B_2}(0)} f_1$, the term with frequency $2f_1$ has the highest amplitude. When

$f_2 < \sqrt{J_{2B_2}(0)} f_1$, the term with frequency $f_1 - f_2 - (1 + B_1/U_1)/2\pi$ has the highest amplitude. The decision boundary between these two modes is $f_2 = \sqrt{J_{2B_2}(0)} f_1$. Since B_2 has a small value, $\sqrt{J_{2B_2}(0)}$ is slightly smaller than 1, the analysis agrees with the numerical results in Fig. 5.

We lastly went back to the equation of motion $m\ddot{x}_2 = -F_2 + C_D(\dot{x}_2)^2$, which is a forced damped system. The dominant frequency of forcing term F_2 determines the frequency of solution x_2. When the motion of the follower is dominated by its own transverse oscillations, the frequency of x_2 is $2f_2$. When sensing flow velocity, similar to the first simplified case described in Sec. III-A, the dominant frequency of the signal is f_2 given that the amplitude of both swimmers is the same. On the other hand, when the interaction term dominates the motion of the follower, the frequency of the follower's motion ($f_1 - f_2$) and the spatial pattern of the wake add up. Thus, the dominant frequency is $f_1 +$ constant.

IV. SLIDING MODE CONTROLLER DESIGN

Our goal is to design a controller that stabilizes two uncoordinated swimmers in a cohesive school formation. Via the analysis in Sec.III, we found that the follower can extract information about the frequency of the leader f_1 based on only local flow sensing, but our sensing algorithm does not provide an accuracy measurement of f_1. Through analyzing the passive pairs in Sec. II, we know that a subtle mismatch in frequency leads to unstable formations. Thus, instead of sensing once and matching frequency, we applied a controller that involves periodic sensing and adjusting frequency.

From Sec. III, both flow velocity at the position of the follower and the follower's swimming velocity contain information about the leader's frequency. However, when sensing its own swimming velocity, $2f_2$ and $f_1 - f_2 +$constant creates ambiguity. Thus, we used flow velocity as the sensory cue, and designed a sliding mode controller as follows,

$$f_2 = \begin{cases} f_2 - c_1, & |f_2 - f_s| \le c_3 \\ f_s - c_2, & |f_2 - f_s| > c_3 \end{cases}, \tag{8}$$

where c_1, c_2, c_3 are constants. This controller can be understood intuitively as follows. When the sensed frequency f_s is close to the follower's own frequency (the difference is less than a threshold c_3), it means that $f_2 > f_1$, thus we need to decrease f_2. However, since we don't know the value of f_1, we apply the controller to decrease f_2 by a small step until f_s is not close to f_2. When this happens, it means that f_s is f_1 plus a constant. Thus, the controller switches f_2 to f_s minus a constant c_2. In this study, these constants are chosen as $c_1 = 0.03$, $c_2 = 0.2$, $c_3 = 0.1$. Since we need to apply a Fourier series expansion to the signal, we apply the controller intermittently. We chose the time interval to be $5/f_1$.

This controller guides the follower to form a stable limit cycle with the leader. Fig. 6A shows the time evolution of the scaled distance with different initial conditions. Simulations show that limit cycles exist in multiple spatial locations, which is different from the passive limit cycle, which is a global attractor. This implies that larger inline schools can be constructed based on this frequency controller, where different uncoordinated swimmers stay at different distances. We plotted the scaled distance over frequency ratio f_2/f_1 in Fig. 6B for one of these trajectories, in which black dots show when the controller is applied.

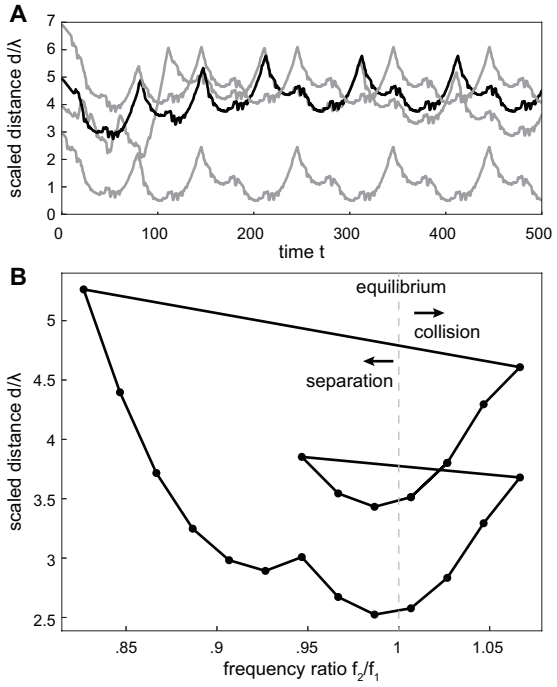

Fig. 6. Controller behavior. **A.** Scaled distance as a function of time with different initial conditions. **B.** Scaled distance over frequency ratio for the case plotted by black line in **A.**. Black dots show where the controller changes frequency f_2. Behavior of the swimmer is plotted in SI movie.

V. CONCLUSIONS

We developed a frequency controller to achieve stable formation for uncoordinated swimmers based on local flow sensing. The follower adjusts its frequency to match the frequency of the leader. However, because the sensed frequency f_s does not accurately represent the frequency of the leader, the follower needs to apply sensing and control periodically and form a limit cycle instead of staying at a stable equilibrium point. This work suggests that when a subset of fish in a school decide to accelerate or decelerate their motion via modulating their tailbeat frequency, other fish in the school can "feel" the change with only local flow sensing. Although we only studied this controller in a school of two swimmers, it can be applied to larger inline schools. This information propagation can be equally applied to robotic fish swarms, in which telecommunication is limited in underwater environments.

The analysis presented in this paper is relevant to problems that share similar features. The challenge of the problem in question comes from two aspects. Initially, the issue arises from the time delay, which intertwines the equations of motion for both swimmers. In this research, we analytically

determined the leader's average swim speed while disregarding its oscillatory behavior. This approach, a first-order approximation, effectively addresses the time delay, allowing for the separation of the follower's motion. The second challenge involves the nesting of trigonometric functions. Our findings suggest that using the first and second terms of their Fourier series provides a reliable approximation.

In future work, we will consider finite decaying time scale τ, which models the strength of viscous effect physically. Future work would also involve testing and developing this sensory control strategy in numerical and robotic setups. An especially attractive direction is to combine this controller with versatile behavior models. The robustness of the proposed controller needs to be examined under models with different fidelity, like pitching/heaving airfoil, 2d fish and 3d fish [25], [26], [6]. Moreover, the combination of machine learning models and this physics-based model can be explored [27]. Also, this frequency controller, combined with amplitude and phase controller, would achieve fully autonomous control in schooling fish [19].

ACKNOWLEDGMENT

This work is supported by NSF CBET-2100209 and NSF RAISE award IOS-2034043 and ONR grant 12707602 and grant N00014-17-1-2062.

REFERENCES

[1] E. Shaw, "Schooling fishes: the school, a truly egalitarian form of organization in which all members of the group are alike in influence, offers substantial benefits to its participants," *American Scientist*, vol. 66, no. 2, pp. 166–175, 1978.

[2] D. Weihs, "Hydromechanics of fish schooling," *Nature*, vol. 241, p. 241290a0, 1973.

[3] B. L. Partridge and T. J. Pitcher, "Evidence against a hydrodynamic function for fish schools," *Nature*, vol. 279, no. 5712, pp. 418–419, 1979.

[4] Y. Zhang and G. V. Lauder, "Energy conservation by group dynamics in schooling fish," Oct. 2023. [Online]. Available: http://dx.doi.org/10.7554/eLife.90352.1

[5] M. S. Triantafyllou, G. S. Triantafyllou, and D. K. Yue, "Hydrodynamics of fishlike swimming," *Annual review of fluid mechanics*, vol. 32, no. 1, pp. 33–53, 2000.

[6] S. Verma, G. Novati, and P. Koumoutsakos, "Efficient collective swimming by harnessing vortices through deep reinforcement learning," *Proceedings of the National Academy of Sciences*, vol. 115, no. 23, p. 201800923, 2018.

[7] J. C. Liao, D. N. Beal, G. V. Lauder, and M. S. Triantafyllou, "Fish exploiting vortices decrease muscle activity," *Science*, vol. 302, no. 5650, pp. 1566–1569, 2003.

[8] J. C. Liao, "A review of fish swimming mechanics and behaviour in altered flows," *Philosophical Transactions of the Royal Society B: Biological Sciences*, vol. 362, no. 1487, pp. 1973–1993, 2007.

[9] E. T. Lunsford, A. Paz, A. C. Keene, and J. C. Liao, "Evolutionary convergence of a neural mechanism in the cavefish lateral line system," *Elife*, vol. 11, p. e77387, 2022.

[10] S. Taneda, "Experimental investigation of vortex streets," *Journal of the Physical Society of Japan*, vol. 20, no. 9, pp. 1714–1721, 1965.

[11] G. S. Triantafyllou, M. Triantafyllou, and M. Grosenbaugh, "Optimal thrust development in oscillating foils with application to fish propulsion," *Journal of Fluids and Structures*, vol. 7, no. 2, pp. 205–224, 1993.

[12] A. D. Becker, H. Masoud, J. W. Newbolt, M. J. Shelley, and L. Ristroph, "Hydrodynamic schooling of flapping swimmers," *Nature Communications*, vol. 6, p. 8514, 2015.

[13] S. Ramananarivo, F. Fang, A. Oza, J. Zhang, and L. Ristroph, "Flow interactions lead to orderly formations of flapping wings in forward flight," *Phys. Rev. Fluids*, vol. 1, p. 071201, Nov 2016. [Online]. Available: https://link.aps.org/doi/10.1103/PhysRevFluids.1.071201

[14] J. W. Newbolt, J. Zhang, and L. Ristroph, "Flow interactions between uncoordinated flapping swimmers give rise to group cohesion," *Proceedings of the National Academy of Sciences*, vol. 116, p. 201816098, 2019.

[15] ——, "Lateral flow interactions enhance speed and stabilize formations of flapping swimmers," *Physical Review Fluids*, vol. 7, no. 6, p. L061101, 2022.

[16] X. Zhu, G. He, and X. Zhang, "Flow-mediated interactions between two self-propelled flapping filaments in tandem configuration," *Physical review letters*, vol. 113, no. 23, p. 238105, 2014.

[17] G. Arranz, O. Flores, and M. García-Villalba, "Flow interaction of three-dimensional self-propelled flexible plates in tandem," *Journal of Fluid Mechanics*, vol. 931, 2022.

[18] S. Heydari and E. Kanso, "School cohesion, speed and efficiency are modulated by the swimmers flapping motion," *Journal of Fluid Mechanics*, vol. 922, p. A27, 2021.

[19] S. Heydari, H. Hang, and E. Kanso, "Mapping spatial patterns to energetic benefits in groups of flow-coupled swimmers," *(under review at Elife)*, 2024.

[20] L. Li, M. Nagy, J. M. Graving, J. Bak-Coleman, G. Xie, and I. D. Couzin, "Vortex phase matching as a strategy for schooling in robots and in fish," *Nature Communications*, vol. 11, no. 1, p. 5408, 2020.

[21] G. Li, D. Kolomenskiy, H. Liu, B. Thiria, and R. Godoy-Diana, "Hydrodynamical fingerprint of a neighbour in a fish lateral line," *Frontiers in Robotics and AI*, vol. 9, 2022.

[22] A. J. Smits, "Undulatory and oscillatory swimming," *Journal of Fluid Mechanics*, vol. 874, 2019.

[23] T. Wu, "Hydromechanics of swimming propulsion. part 1. swimming of a two-dimensional flexible plate at variable forward speeds in an inviscid fluid," *Journal of Fluid Mechanics*, vol. 46, no. 2, pp. 337–355, 1971.

[24] D. Floryan, T. Van Buren, C. W. Rowley, and A. J. Smits, "Scaling the propulsive performance of heaving and pitching foils," *Journal of Fluid Mechanics*, vol. 822, pp. 386–397, 2017.

[25] H. Hang, S. Heydari, J. H. Costello, and E. Kanso, "Active tail flexion in concert with passive hydrodynamic forces improves swimming speed and efficiency," *Journal of Fluid Mechanics*, vol. 932, 2022.

[26] J.-H. Seo and R. Mittal, "Improved swimming performance in schooling fish via leading-edge vortex enhancement," *Bioinspiration & Biomimetics*, vol. 17, no. 6, p. 066020, 2022.

[27] Y. Jiao, F. Ling, S. Heydari, N. Heess, J. Merel, and E. Kanso, "Learning to swim in potential flow," *Physical Review Fluids*, vol. 6, no. 5, p. 050505, 2021.